SIMULATION OF BOTDA AND RAYLEIGH COTDR SYSTEMS TO STUDY THE IMPACT OF NOISE ON DYNAMIC SENSING

Adam Funnell[1], Xiaomin Xu[1], Jize Yan[1*], Kenichi Soga[1]

[1]*Department of Engineering, University of Cambridge, Cambridge CB2 1PZ, UK*

**E-mail: jy242@cam.ac.uk*

ABSTRACT: Dynamic distributed sensing of strain and temperature is the key for real-time structural health monitoring (SHM) across a wide range of geo-engineering challenges, for which Brillouin Optical Time Domain Analysis (BOTDA) and Rayleigh Coherent Optical Time Domain Reflectometry (COTDR) are promising candidates. A noise model with specific parametric simulation of the two systems has been developed. Noise in both laser(s) and detector is independently simulated to identify the key noise sources. In this simulation, although averaging can significantly enhance the signal-to-noise ratio (SNR) in the two systems, it is a barrier to dynamic sensing due to its time-consuming accumulation procedure. The sequence of averaging in the signal processing workflow can vary the SNR for the two systems. The system components should be optimized to reduce the averaging times to achieve the required system specifications, especially the dynamic sensing performance.

KEYWORDS: dynamic sensing, noise simulation, BOTDA, COTDR, laser fluctuation, detection, averaging

1 INTRODUCTION

Distributed fibre optic sensing (DFOS) systems can sense temperature and strain information over very long distances with high accuracy [1, 2]. This allows for effective structural health monitoring (SHM) of a wide range of geo-engineering projects, facing challenges such as aging or nearby construction works [3]. Recent progress in DFOS has demonstrated very high spatial, strain and temperature resolutions [4]. However progress is slow in developing a long-distance dynamic sensing system, despite clear industrial demand for real-time SHM.

BOTDA (utilizing the amplitude of stimulated Brillouin scattering) and COTDR (utilizing the amplitude and phase of Rayleigh backscatter) systems have already been demonstrated for distributed long-distance sensing [4, 5]. However, there are barriers to achieving dynamic performance using these systems, such as the need to sweep through the overall frequency span to find the Brillouin frequency shift (or Rayleigh equivalent in the COTDR system); the need for large numbers of ensemble averages to increase the SNR; and the time taken for the pulse to transit the fibre (in very long-distance sensing) [6]. Novel methods have been developed elsewhere to reduce the time taken for frequency sweeping [7, 8], and this work concentrates on the reduction of ensemble averaging time through careful opto-electronic component selection and the choice of methods for processing the received data.

Many attempts have been made to model BOTDA and COTDR systems [9, 10]; however these models generally use only the additive white Gaussian noise (AWGN) model applied at the end of pulse transmission simulations. This work seeks to more accurately replicate real-world noise sources, using appropriate probability distributions, and to use the results to suggest optimal components for best performance. There are two major noise contributions within laser sources: phase noise (also known as laser linewidth) and relative intensity noise (RIN). Laser linewidth measures the deviation of the emitted light wave from an ideal sine wave of specified frequency. RIN measures the deviation of the laser's power from a nominal output optical power (usually the maximum) when held at a constant input power (e.g. constant current for semiconductor diode lasers). These deviations mainly come from spontaneous emission within the laser cavity, a naturally random process. A third noise source in DFOS systems is the thermal and shot noise in detection components. In both the BOTDA and COTDR simulation models, it is assumed that the noise from the photo-detector and any photonic pre-amplification can be specified as the equivalent optical power noise floor of a single AWGN source.

2 METHOD

The Brillouin system model is based on the mathematical derivations of Minardi et al. [11, 12] and implemented in MATLAB for a two-laser stimulated Brillouin emission system. A continuous wave probe laser and pulsed pump laser are simulated at opposite ends of a fibre. A steady state solution is found for the power of the pump and probe laser propagation through the fibre, before the application of a novel equation derived from the three wave mixing equations to find the Brillouin gain for each frequency difference (ω) between pump and probe lasers [11]:

$$G(z,\omega) = E_s^{CW}(z) \cdot \left(\mathbf{E_p}(0,\omega) \otimes \frac{\mathbf{E_p}(0,\omega)}{\Gamma_1 - j(\Delta(z)+\omega)} \right)$$

where G(z,ω) is Brillouin gain, $E_s^{CW}(z)$ the Stokes laser amplitude and $E_P(z,\omega)$ the probe laser amplitude, with other constants as derived in [11]. This process is then repeated whilst the frequency difference between pump and probe lasers is varied in steps across the whole range.

This raw data has the constant background Brillouin scatter level subtracted, which otherwise forms a "DC offset" to the scatter signal which varies through the fibre. A Lorentzian fit is applied across the frequency span by cross-correlation [13], before conversion of the frequency shift at the fitted peaks to strain values using an empirical formula.

The Rayleigh COTDR system uses a single laser, and measures the amplitude and phase of backscatter from the fibre back to the laser source to infer strain and temperature information. This model is based on the mathematical derivations of several groups [9, 10, 14, 15]. The model considers the fibre to be split into many tiny sections of partially reflecting mirrors, with random phase and intensity reflected at each. The total backscattered power P(z) can be calculated as follows [9]:

$$\begin{aligned} P(z) &= |E(z)|^2 \\ &= \left[\sum_{i=1}^{M} a_i \exp(j\Omega_i)\right]\left[\sum_{i=1}^{M} a_i \exp(-j\Omega_i)\right] \\ &= \sum_{m=1}^{M}\sum_{n=1}^{M} a_m a_n \exp\left[j\left(\Omega_m - \Omega_n\right)\right] \end{aligned}$$

for backscatter amplitude E(z) at distance z along the fibre, M individual phase mirrors, a_i and Ω_i the amplitude and phase response at each mirror i respectively, with renumbering to m and n for mathematical simplicity.

The Rayleigh response of the fibre is assumed constant over time without external influences. However, the phase changes depend on both incident frequency and refractive index. Changes in strain or temperature can change the local refractive index, but this effect can be "cancelled out" by a laser frequency change i.e. [9]

$$\Omega_m - \Omega_n = 4\pi f_0 \Delta L_{mn} n_0 / c$$

where L_{mn} is the distance between adjacent scattering centres and all other symbols take their usual meanings.

The frequency shift that gives the same phase change and thus backscatter pattern as the strain/temperature perturbed section can be found using a cross-correlation technique between the perturbed and unperturbed cases [10]. The fibre strain can then be recovered using an empirical formula [14].

To model laser linewidth, a Lorentzian model is used [16]. This is implemented via the ratio of two Gaussian distributions applied to the frequency of the laser source. To model the laser RIN, it is assumed that the laser power fluctuates at the source with a Gaussian profile. A percentage value can be specified (as generally given by laser diode manufacturers), and this can be converted to the width of Gaussian required for accurate modelling. To model detector noise, a white Gaussian noise floor (converted to an optical power equivalent) is specified at the detector; this value incorporates the noise from any additional optical or electrical pre-amplification.

Further assumptions made in the systems modelled are a lack of polarisation sensitivity (achievable in practice through use of a polarisation scrambler with ensemble averaging); no amplification in the fibre and thus no optical noise generated along the length of the fibre; and linear attenuation (due to Rayleigh scattering and absorption) through the fibre, with no splicing losses.

Throughout this work, the SNR for each system has been calculated as follows: the mean difference between the optical signal power as measured by the detector including the specified noise types, and the optical power measured for a simulated ideal case with zero noise has been calculated, with power measurements filtered to a 0.1nm/12GHz bandwidth. The ratio of this power difference and the mean signal power was taken and then averaged across all frequencies within the sweep for a given set of components. No averaging was applied unless stated.

3 RESULTS

3.1 General observations

3.1.1 Variable ensemble averaging limits

Ensemble averaging of noisy data from DFOS systems can enhance the final SNR, however the enhancement can reach a limit for any given system. Figure 1 shows an example for BOTDA systems of various SNRs before averaging. These simulations considered the Time Domain Spatial Resolution (TDSR), defined as the distance equivalent of the 10-90% rise time of strain data for a step change in strain in the simulated fibre. Although the pulse width provides a fundamental limit to spatial resolution, a poor system SNR will increase this limit. A smaller TDSR therefore corresponds to a larger SNR. Figure 1 shows that systems of various SNRs all converge to the same limit, and that further averaging after reaching that point provides no overall benefit to the final results of the system – a steady state of best performance.

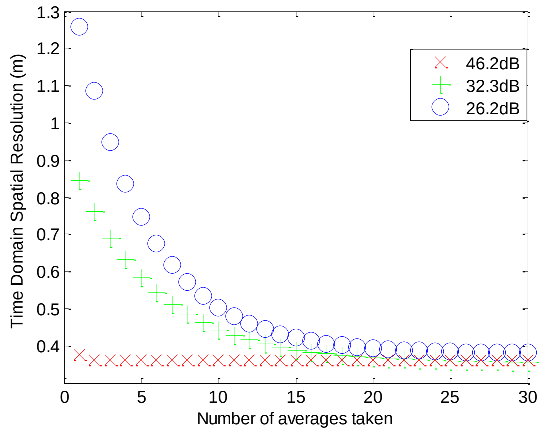

Figure 1: Time domain spatial resolution after ensemble averaging for various SNR BOTDA systems – SNRs quoted are before averaging.

It is proposed that for dynamic data acquisition, the number of averages required should be found through an algorithm which seeks the minimum averages required to reach the steady state of best performance under the prevailing circumstances, rather than always requiring a fixed number. For example, temperature variations of the laser cavity or photodiode could result in performance changes over time, requiring different amounts of averaging.

3.1.2 Ensemble averaging position within Digital Signal Processing (DSP)

The Digital Signal Processing (DSP) described in section 2 above is shown as a flow chart for each system in figure 2. The averaging technique could be applied at any stage of the signal processing, however table 1 shows the SNR achieved after 200 averages for both systems dependent on the sequence in the DSP flow.

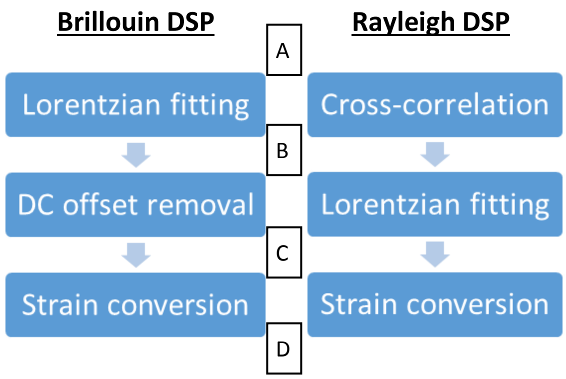

Figure 2: The signal DSP flows for both BOTDA and Rayleigh COTDR systems, as derived in section 2.

It is shown in table 1 that the earlier in the signal flow that averaging is performed, the better the final SNR. Thus the averaging should be performed on raw data at the photo-detector to minimise averages required (and thus time taken) to enhance SNR.

Table 1 SNR at various stages of DSP, at points shown in figure 5, after 200 averages, assuming 1MHz linewidth, -40dBm detector noise floor and 3% RIN.

DSP Position	Brillouin SNR (dB)	Rayleigh SNR (dB)
A	24.1	4.98
B	22.0	4.20
C	20.3	3.83
D	20.3	3.83

3.2 BOTDA Results

3.2.1 Brillouin System Parameters

For BOTDA, a frequency sweep step size of 5MHz over a 200MHz range was used to gather data on a 50m fibre with a 10με strain perturbation across 1m at its centre. It is also assumed for this BOTDA simulation that laser noise sources apply identically to both pump and probe lasers.

3.2.2 Laser Linewidth

Figure 3 shows the change in SNR as the laser linewidth is varied, at constant 3% RIN and -40dBm detector noise floor. The flat region below 0.1MHz demonstrates that below that turning point, other noise sources dominate rather than the laser linewidth. Each laser pulse emitted is considered identical, with the same total energy, and when this energy is spread over a greater range of the spectrum due to a larger linewidth, the energy of the signal at the desired frequency will be weaker. To maintain low cost components yet high SNR, and thus least averaging times and faster signal processing, a linewidth of 0.1MHz is recommended for BOTDA system.

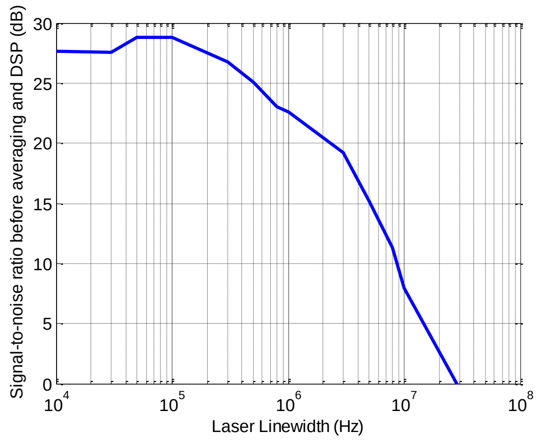

Figure 3: SNR as a function of laser linewidth for a BOTDA system.

3.2.3 Laser Relative Intensity Noise (RIN)

Figure 4 shows the change in SNR as the laser RIN is varied, at constant 1MHz linewidth and -40dBm detector noise floor. There is far less variation of SNR with RIN as with other noise sources, because the RIN causes small perturbations to intensity without affecting the frequency. Therefore, the overall Brillouin frequency response is reasonably well preserved.

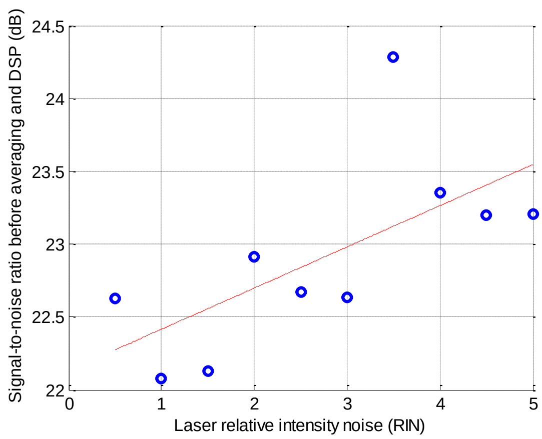

Figure 4: SNR as a function of laser RIN (%) for a BOTDA system.

Since the RIN distribution is assumed to be Gaussian on both pump and probe laser sources, on average the RIN could cancel out due to opposing positive and negative intensity fluctuations on each laser, that effectively removes any overall power variation within the fibre when both pump and probe contributions are summed. For instance, a simultaneous increase in pump power and decrease in probe power gives the same total instantaneous power within the fibre – statistically this should occur for 50% of samples due to the Gaussian distribution of RIN.

3.2.4 Receiver/Detector Noise

Figure 5 shows the change in SNR as the noise floor of the detector is varied, with constant 1MHz laser linewidth and 3% RIN. The linearly increasing section demonstrates the dominance of thermal and shot noises at the detector over all other noise sources for a noise floor of -40dBm or greater, whilst the flat region for noise floors <-40dBm implies that other noise sources are now the limiting factor. For this BOTDA system, if seeking high SNR to minimise averaging time, there would be no benefit to use an expensive low noise floor detector below -40dBm without improving other components.

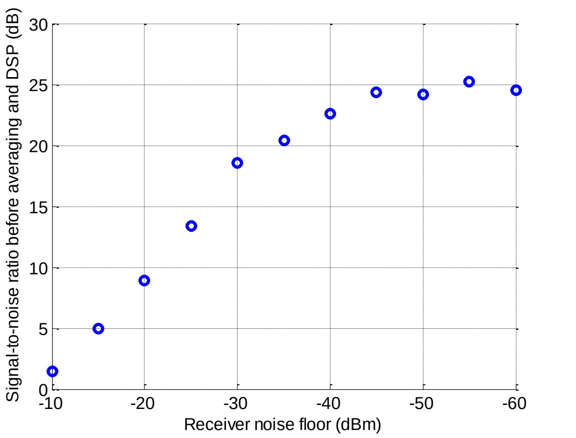

Figure 5: SNR for varied receiver noise floor in equivalent optical power (dBm) in a COTDR system

3.3 Rayleigh COTDR Results

3.3.1 System Parameters

For COTDR, a frequency sweep step size of 5MHz over a 200MHz range was used to gather data on a 50m fibre with a 1με strain perturbation across 1m at its centre. A smaller strain perturbation was used with Rayleigh COTDR than the BOTDA in section 3.2 due to the better resolution achievable with Rayleigh, else a substantially greater frequency sweep size would have been required [9].

3.3.2 Laser Linewidth

Figure 6 shows the change in SNR as the laser linewidth is varied, at constant 3% RIN and -40dBm detector noise floor. Similarly to the BOTDA system, a limit is found below which linewidth is no longer the dominant noise source, however this limit is now 10MHz. Despite most coherent optical systems relying on low phase noise, COTDR has been shown here to have greater linewidth tolerance than BOTDA. In practical systems and in this simulation, the scattering centres are spaced closer together than the spatial length of the pulse. This means that single pulses contain contributions from multiple scattering locations. Thus this system displays a level of inherent averaging, as the linewidth can effectively average out over the entire pulse length. However for large linewidths (10MHz or more) this effect is less prominent, due to the small number of scattering centres simulated within each pulse duration in this system.

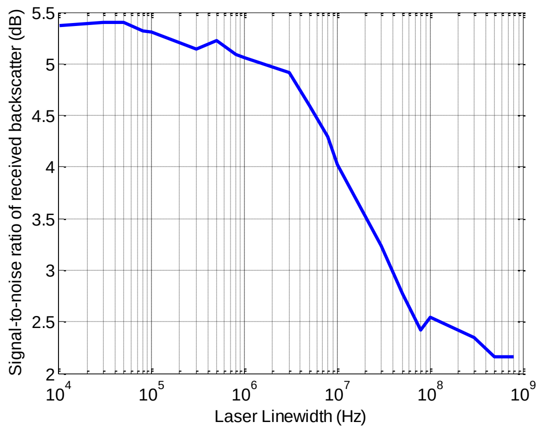

Figure 6: SNR for varied laser linewidth in a COTDR system

3.3.3 Laser Relative Intensity Noise (RIN)

Figure 7 shows the change in SNR as the laser RIN is varied, at constant 1MHz linewidth and -40dBm detector noise floor. As with the BOTDA system, the variation of SNR is low, <0.5dB over the 0-5% range studied, for the same reasons as given in section 3.2.2. This value refers to the optical signal at the detector only, but the cross-correlation step of the DSP which follows the detection is also highly resistant to small changes in instantaneous intensity [17], searching only for localised matches in intensity pattern over a patch, thus showing even further tolerance of RIN.

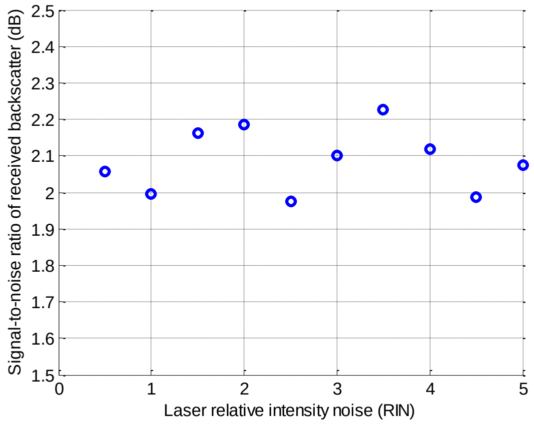

Figure 7: SNR for varied laser RIN in a COTDR system

3.3.3 Receiver/Detector Noise

Figure 8 shows the change in SNR as the detector noise floor is varied, at constant 1MHz linewidth and 3% RIN. As with the BOTDA system there is a linear relation between the receiver noise floor and overall SNR, up until a point where the noise floor (here -60dBm) is no longer the noise source of greatest prominence.

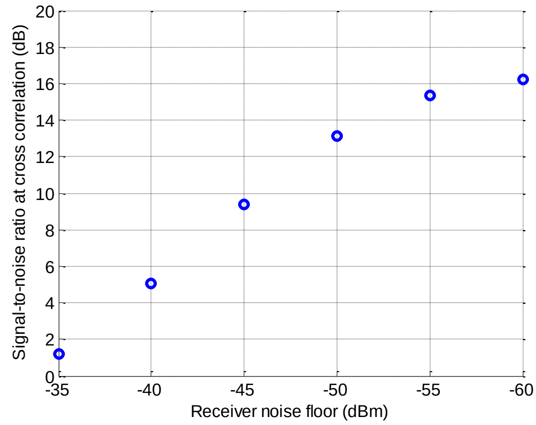

Figure 8: SNR for varied receiver noise floor in equivalent optical power (dBm) in a COTDR system

4 CONCLUSIONS

BOTDA and Rayleigh COTDR fibre-optic sensing systems show great promise in structural health monitoring for geo-engineering, but have long data acquisition times due to the numerous ensemble averages required to improve poor SNRs. In a typical fibre optic sensing system, careful component choice can improve the SNR significantly to improve the data acquisition quality, reduce the ensemble averages required and thereby enhance the sensing speed to a dynamic level.

Ensemble averaging increases SNR to a limit in any given system; the number of ensemble averages required could be varied according to prevailing system parameters, to increase data acquisition speed. An algorithm could be found to measure the properties of the DFOS system and adjust averaging to increase measurement speed, working towards dynamic analysis.

A model has been built to analyse the contributions of multiple noise sources in a typical system, and results for a particular simulated system discussed. Laser linewidth and receiver thermal/shot noise are found to be more dominant over laser relative intensity noise when considering components for both BOTDA and Rayleigh COTDR systems. Reducing laser linewidth is more important in a BOTDA than a Rayleigh COTDR system. With appropriate choice of components, higher SNRs can be achieved with less averaging, meaning faster data acquisition for dynamic sensing.

ACKNOWLEDGMENTS:

This project was carried out under the UCL-Cambridge Centre for Doctoral Training in Photonic Systems Development, with funding from EPSRC (EP/G037256/1) gratefully acknowledged. The funding from Cambridge Centre for Smart Infrastructure and Construction is acknowledged.

REFERENCES:

[1] Z Qin, T Zhu, and X Bao, 2011. High frequency response distributed vibration sensor based on all polarization-maintaining configurations of phase-otdr. IEEE Photonics Technology Letters, 23: 1091-1093.

[2] Z Qin, L Chen, and X Bao, 2012. Wavelet denoising method for improving detection performance of distributed vibration sensor. IEEE Photonics Technology Letters, 24: 542-544.

[3] Branko Glisic, 2013. Distributed Fiber Optic Sensing Technologies and Applications – An Overview. American Concrete Institute Special Publication, 292: 1-18.

[4] Xiaoyi Bao and Liang Chen, 2012. Recent Progress in Distributed Fiber Optic Sensors. Sensors, 12: 8601:8639.

[5] Luca Palmieri and Luca Schenato, 2013. Distributed Optical Fiber Sensing Based on Rayleigh Scattering. The Open Optics Journal, 7: 104:1274

[6] Yair Peled, Avi Motil, Lior Yaron and Moshe Tur, 2012. Fast and distributed Brillouin time domain analysis of optical fibers. OFS2012 22nd International Conference on Optical Fiber Sensors.

[7] Romeo Bernini, Aldo Minardo, and Luigi Zeni, 2009. Dynamic strain measurement in optical fibers by stimulated brillouin scattering. Optics Letters, 34: 2613-2615.

[8] M. Taki, Y. Muanenda, C. J. Oton, T. Nannipieri, A. Signorini, and F. Di Pasquale, 2013. Cyclic pulse coding for fast botda fiber sensors. Optics Letters, 38: 2877-2880.

[9] Yang Zhi, Shi Pengxiang, and Li Yongqian, 2011. Research on cotdr for measuring distributed temperature and strain. 2011 Second International Conference on Mechanic Automation and Control Engineering (MACE).

[10] Yongqian Li, Rongwei Li, and Zhi Yang, 2010 Coherent otdr for measuring distributed temperature and strain with high resolution in km-long fiber. 2010 International Conference on Intelligent Computation Technology and Automation.

[11] Aldo Minardo, Romeo Bernini, and Luigi Zeni, 2007. Stimulated brillouin scattering modelling for high-resolution, time-domain distributed sensing. Optics Express, 15: 10397-10407.

[12] Aldo Minardo, Romeo Bernini, and Luigi Zeni, 2011. Numerical analysis of single pulse and differential pulse-width pair botda systems in the high spatial resolution regime. Optics Express, 19: 19233-19244.

[13] Mohsen Amiri Farahani, Eduardo Castillo-Guerra and Bruce G. Colpitts, 2013. A Detailed Evaluation of the Correlation-Based Method Used for Estimation of the Brillouin Frequency Shift in BOTDA Sensors. IEEE Sensors Journal, 12: 4589:4598.

[14] Wenhai Li, Xiaoyi Bao, Yun Li, and Liang Chen, 2008. Differential pulse-width pair botda for high spatial resolution sensing. Optics Express, 16:21616-21625.

[15] Ryosuke Shimano, Yuta Iitsuka, Kenya Kubota, and Yahei Koyamada, 2010. 31-km distributed temperature measurement with very high resolution using coherent-otdr enhanced with bidirectional edfa. 15th OptoElectronics and Communications Conference (OECC2010) Technical Digest.

[16] C.H. Henry, 1982. Theory of the linewidth of semiconductor lasers. IEEE Journal of Quantum Electronics, 18: 259-264.

[17] Yahei Koyamada, Mutsumi Imahama, Kenya Kubota and Kazuo Hogari,2009. Fiber-Optic Distributed Strain and Temperature Sensing With Very High Measurand Resolution Over Long Range Using Coherent OTDR, Journal of Lightwave Technology, 27: 1142-1146.